

Open-jet boundary-layer processes for aerodynamic testing of low-rise buildings

Hamzeh Gol-Zaroudi and Aly-Mousaad Aly*

Department of Civil and Environmental Engineering, Louisiana State University, 3240M Patrick F. Taylor Hall,
Baton Rouge, LA 70803, USA

(Received August 25, 2016, Revised June 18, 2017, Accepted July 31, 2017)

Abstract. Investigations on simulated near-surface atmospheric boundary layer (ABL) in an open-jet facility are carried out by conducting experimental tests on small-scale models of low-rise buildings. The objectives of the current study are: (1) to determine the optimal location of test buildings from the exit of the open-jet facility, and (2) to investigate the scale effect on the aerodynamic pressure characteristics. Based on the results, the newly built open-jet facility is well capable of producing mean wind speed and turbulence profiles representing open-terrain conditions. The results show that the proximity of the test model to the open-jet governs the length of the separation bubble as well as the peak roof pressures. However, test models placed at a horizontal distance of $2.5H$ (H is height of the wind field) from the exit of the open-jet, with a width that is half the width of the wind field and a length of $1H$, have consistent mean and peak pressure coefficients when compared with available results from wind tunnel testing. In addition, testing models with as large as 16% blockage ratio is feasible within the open-jet facility. This reveals the importance of open-jet facilities as a robust tool to alleviate the scale restrictions involved in physical investigations of flow pattern around civil engineering structures. The results and findings of this study are useful for putting forward recommendations and guidelines for testing protocols at open-jet facilities, eventually helping the progress of enhanced standard provisions on the design of low-rise buildings for wind.

Keywords: atmospheric boundary-layer; building aerodynamics; low-rise buildings; open-jet testing; scale issues; separation bubble; turbulence; wind loads; wind pressure measurement; wind tunnels

1. Introduction

1.1 Background

Engineers are always interested in understanding the behavior of structures under the effects of various loads that can have the possibility to influence the response of a structure during its life. Wind forces are considered as complicated dynamic loads that can threaten safety of structures if their effects are underestimated; therefore, it is crucial to properly simulate and assess wind effects on structures in order to optimally design resilient buildings that can maintain functionality and vitality in the face of natural disasters caused by stormy wind conditions. Considering the climate

*Corresponding author, Assistant Professor, E-mail: aly@LSU.edu

change consequences, the patterns of extreme winds and hurricane occurrence have been altered (Knutson *et al.* 2010, Mann and Emanuel 2006). As a tangible result, wind loads are being much more highlighted in the analysis and design of buildings, especially in hurricane vulnerable regions. To put it in perspective, in most parts of the United States, especially in southern parts, it has yearly been widespread that wind storms severely hit and damage buildings. These buildings are mostly light low-rise buildings constructed from wooden materials with different aerodynamic performance compared to high-rise buildings. On this basis, in order to propose mitigation solutions to improve the performance of low-rise buildings for wind, it is crucial to properly simulate near-surface atmospheric boundary-layer (ABL) and flow characteristics around buildings.

1.2 Review

Since the past decades, wind tunnel modelling has been widely used as a useful technique in order to estimate wind loads on buildings. However, in the case of low-rise buildings, it has been always a challenge in the wind tunnel to properly simulate wind effects due to the lack of capability in turbulence modelling at a reasonably large scale. In addition, testing a low-rise building in a wind tunnel will cause an issue with the Reynolds number that can be far different from the one in nature (Aly 2014). To cope with these issues, efforts have been made to investigate the appropriateness of alternative tools, for instance implementing computational fluid dynamic (CFD) simulations for wind engineering problems. Even with the current CFD programs are being improved rapidly, it is still a challenge for accurately simulating peak pressures on residential buildings, even with supercomputers (Cochran and Derickson 2011). The CFD showed its potential application when implemented in the design of an open-jet simulator where the results of a preliminary CFD simulations are very similar to those obtained from the experiment (Aly *et al.* 2013, 2011, Aly and Gol-Zaroudi 2017)

Although recent advancements in mathematics have revolutionized computational modelling, still experimental wind engineering has an important role due to the fact that wind loads depend on structures' shape, their location, terrain topography, among other factors, that makes direct measurements of these loads under real flow conditions indispensable. In addition, computational modelling can be very time consuming and may require experimental validations.

Although there are many research studies conducted on the determination of flow characteristics by means of laboratory tests, especially in boundary-layer wind tunnels, there is still a major gap in research studies on the flow simulation and calibration in open-jet facilities which needs further investigations.

Aly *et al.* (2011) studied the wind flow management and devices for the wind field simulation of 12-fan Wall of Wind (WoW) facility. They determined the optimal scale of the test model and its optimal distance from the WoW contraction exit. Also, adjustable planks mechanism has been proposed in order to generate different wind speed profiles in accordance to the desirable terrain characteristics.

Aly *et al.* (2011) proved the capability of open-jet tests to achieve reasonable roof pressure for low-rise buildings under relatively high corresponding tunnel blockage ratios. Huang *et al.* (2009) investigated the feasibility of application of a small-scale (1:8) WoW model to develop the target wind flow generating devices for full-scale WoW testing in which simulation devices were easier and faster to install and change, and running costs were greatly reduced. They showed that the mean and turbulence characteristics of the flow were improved remarkably through the application of passive devices and active controls.

Recently, the Database-Assisted Design (DAD) methodology was developed (Main and Fritz 2006). Hagos *et al.* (2014) implemented the DAD methodology in order to calculate wind loadings and wind-induced internal forces in buildings. Considering the development of DAD and the recent trend to directly analysis and design buildings for wind loads from sets of measured aerodynamic pressure data, it is indeed crucial to have highly reliable experimentally measured time series of wind pressures on buildings. To this aim, the current paper investigates appropriate simulation of near-surface ABL and wind characteristics within an open-jet facility by defining various test scenarios on small scale low-rise buildings in an open-jet facility that has been recently constructed at the Windstorm Impact, Science and Engineering (WISE) research laboratory, Louisiana State University (LSU). The accuracy of the experimental results are compared with sets of results from wind tunnel available at the National Institute of Standards and Technology (NIST), and University of Western Ontario (UWO) aerodynamics database (NIST 2016). The first target of this study was defined to determine the optimal horizontal distance of building models from the exit of the open-jet facility, and the other motivation was to investigate the scale effect on the flow characteristics around the buildings by conducting experimental tests on two small scale models with the same aspect ratio. A model with the scale of 1:100 from the NIST/UWO database was selected as a benchmark, and the pressure coefficients' time series were extracted accordingly. It was an interest to address which scale can better represent the flow pattern around the building with acceptable resolution for open-jet testing in a practical manner.

1.3 Paper layout

This paper investigates the appropriate simulation of near-surface ABL and wind characteristics in a newly built open-jet facility by testing scale models of low-rise buildings. Section 2 represents the methodology adopted, and explains the details of experimental setup and test scenarios in the open-jet facility. In section 3, the results obtained are presented and discussed in details, with obtained recommendations on the optimal size and location of a test building. A discussion of the main results is presented in Section 4. Section 5 summarizes the main conclusions drawn from this research study.

2. Methodology

As described earlier, the main idea of this research is to investigate the characteristics of simulated wind flow in a new open-jet facility and its effect on small scale low-rise buildings. To this aim, experimental tests have been conducted on two small scale models with the same aspect ratio. The LSU WISE open-jet facility was used for simulating the hurricane-force winds. Fig. 1 presents the main concept of the open-jet testing, and the associated wind profile that was modified based on the characteristics of target terrains. The WISE open-jet was made from simple components, i.e., fans, DC batteries, electric connectors, speed controllers, switches, wooden frame, planks, etc. The facility consists of 15 fans in a 3×5 array. It has a test section with dimensions of 0.91 m height and 1.68 m width that can produce a maximum sustained wind flow with speed up to 15 m/s. It is also possible to test wind-driven rain within the system after making some adjustments. Using the adjustable planks mechanism, it is possible to generate different wind velocity profiles in accordance to a desirable terrain characteristics (Aly and Chokwitthaya 2014, Aly and Gol-Zaroudi 2017).

Two models of a low-rise building having the same aspect ratio but different scales of 1:15, and

1:22, were created to be tested in the open-jet facility. The dimensions and the corresponding blockage ratios of the test models are presented in Table 1. The prototype building has dimensions of 13.72 m×9.14 m×3.96 m. The small scale models are made of 2.5 mm and 5 mm thick sheets of acrylic plastic as shown in Fig. 2. It was planned to have a unique pattern for pressure taps' distribution around the building for the two scale models similar to the NIST model in order to make it possible having an apple-to-apple comparison for the pressure distribution on the surface of the models. Therefore, 206 pressure taps based on the pattern described in Ho *et al.* (Ho *et al.* 2003) are installed in order to monitor and obtain the distribution of the simultaneous time varying surface pressure on the roof and sides of each model as shown in Fig. 3. The definition of the wind direction is also designated in Fig. 3. It should be noted that the building model that is tested and introduced by NIST database has a very mild and negligible slope of ¼:12 for the gable roof which is neglected in our test models, and we considered models with a flat roof (zero roof slope).

In order to build the scale models with tap pattern shown in Fig. 3, each tap was connected to Scanivalve pressure scanners by using a 550 mm length flexible Urethane tubing (URTH-063 of Scanivalve Corp. (Scanivalve 2016)). This tubing length is selected based on the recommendation by Ho *et al.* (2003). Ho *et al.* (2003) compared the response spectrum of the measured signal when the tubes were used and when they were not used, i.e., the sensors are directly applied on the surface of models. They came up with a range of length for tubing system that does not negatively affect the acceleration response of the tubing system. In Fig. 2(c), the pressure taps and Urethane tubing connected to the scanning modules' connectors are presented. The internal diameter of flexible Urethane tubing was 1.37 mm.

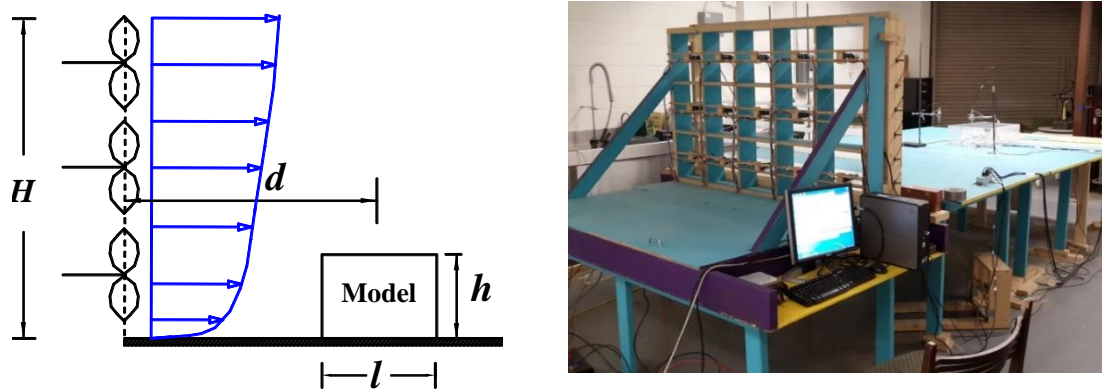


Fig. 1 The open-jet facility. Left: main concept of open-jet testing. Right: open-jet simulator at Louisiana State University

Table 1 Dimensions of small scale models and corresponding wind tunnel blockage ratio

scale	height (m)	width (m)	length (m)	blockage ratio (%)
1:100 (NIST)	0.039	0.091	0.137	--
1:22 (LSU)	0.18	0.41	0.61	10.7
1:15 (LSU)	0.26	0.61	0.91	16.0

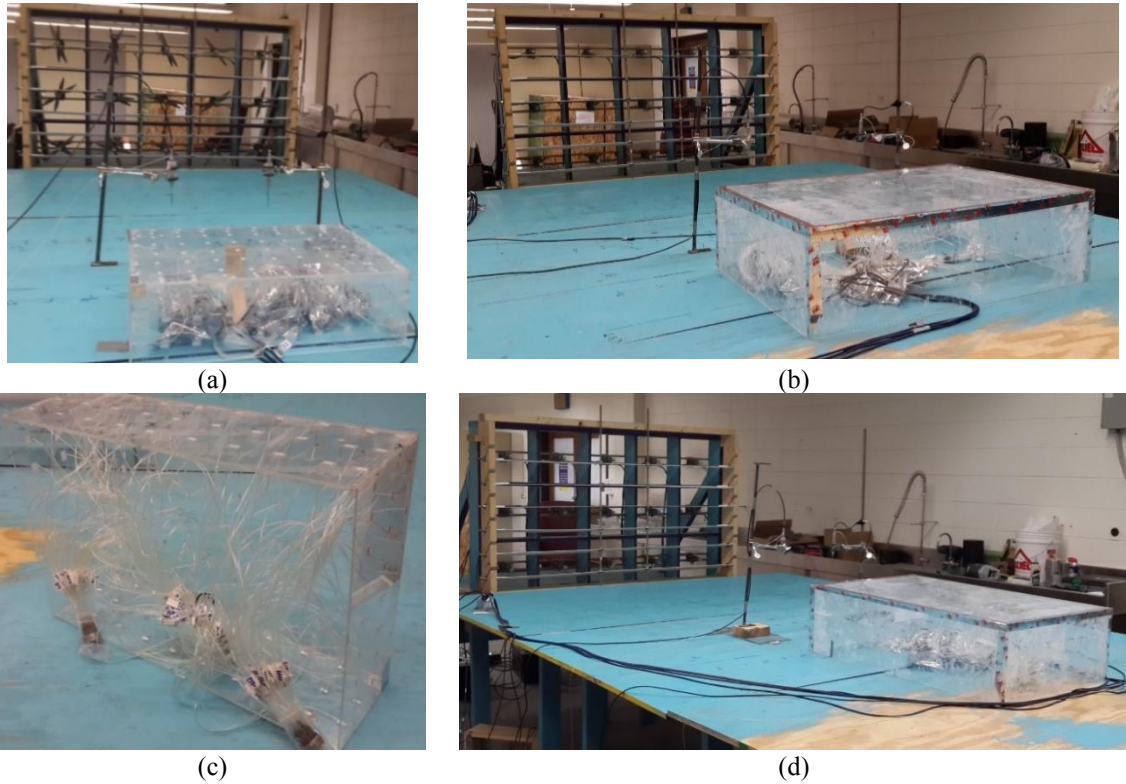


Fig. 2 Test models: (a) The 1:22 scale model test building located in front of LSU WISE open-jet facility at 90° direction angle, (b) The 1:15 scale model, (c) Pressure taps and Urethane tubing connected to the scanning modules' connectors (scale 1:22) and (d) The 1:15 scale model at 0°

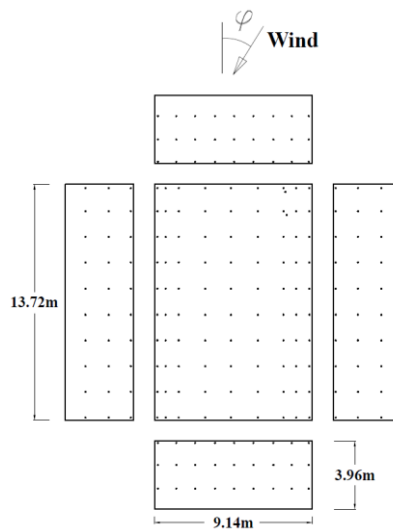


Fig. 3 Exploded view of building with prototype dimensions showing the tap layout and the definition of wind direction angle

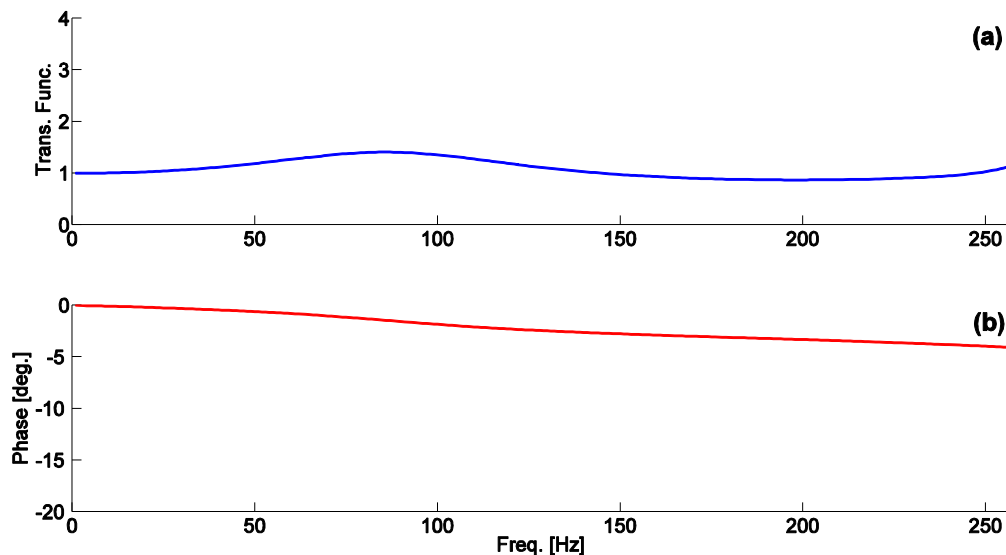


Fig. 4 Frequency response characteristics of the pressure tubing system used in the current study

Fig. 4 shows the frequency response characteristics of the pressure tubing system used in the current study. The transfer functions of amplitude and phase shift are plotted over a range of frequencies of interest. It is worthy to mention that all data were corrected, both magnitude and phase, using the tube transferred function shown on Fig. 4. In fact, the pneumatic connector used in the current study acts in a similar way as the restrictor studied in Ho *et al.* (2003).

Fig. 5 shows a general view of the test rig and sensors used to record and process time histories of velocity and pressure data. One crucial step in the data acquisition procedure was to make sure that the wind speed and wind direction were in accordance to the target ranges. This will be more tangible if it is pointed out that time histories of pressure coefficient are directly dependent on the velocity measurements and turbulence intensity at reference height in the lab. Therefore, wind speed measurement has to be performed with high resolution devices that can catch little changes in wind characteristics; to do so, in the current study Cobra probe technology was used. More details regarding the high tech instruments that were used for experimental setup are presented as follows.

As shown in Fig. 5, there are two Cobra Probes in the experimental setup that were used to monitor the upstream velocity at roof height. The Cobra Probe is a dynamic multi-hole pressure probe for measuring mean and time-varying values of velocity (three-components), pitch and yaw angles, and local static pressure in real time. Turbulence intensity and all six components of Reynolds stresses are also calculated and displayed during the test (Turbulent Flow 2015). Other higher order terms can be calculated from the time-varying data (Turbulent Flow 2015).

As shown in Fig. 5, miniature pressure scanners were used in the experimental setup to measure wind-induced pressures. Two types of pressure scanners that are extremely compact were used: one from ZOC22b series, and three from ZOC33 series (Scanivalve 2016).

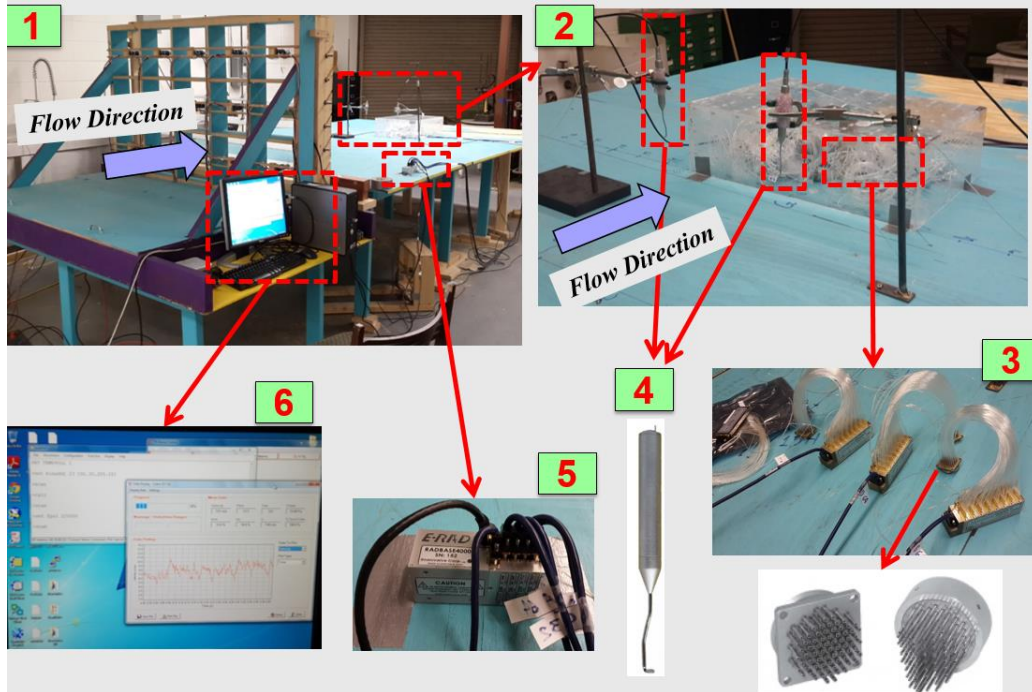


Fig. 5 Experimental setup: 1. general view of the open-jet facility; 2. instrumented test building; 3. ZOC miniature electronic pressure scanning modules, and view of pneumatic connectors; 4. Cobra probe used for measuring mean and fluctuating 3-component velocities and static pressure; 5. RADBASE data acquisition unit; 6. ScanTel and Turbulent Flow software installed on a computer to record and process time histories of pressure and velocities during testing

In order to communicate with the pressure measuring system, Scanivalve Corporation (Scanivalve 2016) wrote the ScanTel utility which is a support program for all modules. It supports communication in ASCII or BINARY formats. It works much like Hyperterminal in order to connect to a product via an IP address. ScanTel was designed for easy Ethernet connections and configuring variables.

Duration of testing: After completing the experimental setup, the pressure signals were obtained from time series with a 625 Hz sampling rate. Each test scenario for 1:22 scale model has been run for a 6-minute duration. The test duration was calculated based on the requirement of equivalence between the reduced frequencies at model scale and at prototype scale, which can be expressed as in Eq. (1)

$$\left(\frac{fl}{u}\right)_m = \left(\frac{fl}{u}\right)_p \quad (1)$$

where f denotes the sampling frequency, u defines the mean wind velocity at a reference height (roof height), and l stands for the characteristic dimension of the structure. The subscripts m and p define the “model” and “prototype” scales as well.

In order to calculate the mean wind velocity in prototype model at roof elevation which is located at 3.96 m, the mean wind velocity at 10 m reference height equals to 17.8 m/s was used. Accordingly, the prototype reference wind speed is:

$u_p(ref) = 17.80(3.96/10)^{0.15} = 15.49 \text{ m/s}$. Therefore, according to Eq. (1), and using $u_m = 8 \text{ m/s}$ as the mean wind speed of testing:

$$f_m/f_p = (u_m/u_p) \times (l_p/l_m) = (8/15.49) \times 22.3 = 11.52.$$

For a full-scale duration of $T_p = 60 \text{ min}$, the laboratory duration is $T_m = T_p/11.52 = 60/11.52 = 5.21 \text{ min}$. Consequently, all tests for 1:22 scale model have been carried out for 6 minutes in order to make sure the stability and repeatability of the peak pressure values are achievable. In a similar way, test durations of 9 minutes were considered for the model with scale of 1:15 corresponding to 1 hour duration in prototype case. It is worthy to mention that the mean wind speeds for the measured time series in the lab in this paper are corresponding to hourly mean speed in real world.

Pressure coefficients: The time history of the pressure coefficient $C_p(t)$ can be obtained from measured instantaneous surface pressures $P(t)$ as follows

$$C_p(t) = \frac{p(t) - \bar{p}_s}{(1/2)\rho U^2} \quad (2)$$

where ρ is the air density, and the U stands for the mean wind speed measured at the reference height (roof height). The term $p(t) - \bar{p}_s$ defines the difference of instantaneous pressure with respect to the mean static pressure. The static pressure was measured during each experiment at a location on the floor, where the dynamic effect of the wind was zero. In wind tunnel testing, this corresponds to the pressure reference on the internal wall of the tunnel. Obviously the two scenarios are different. A total static negative pressure is expected in the tunnel, while the static pressure in open-jet testing corresponds to the atmospheric pressure at the test location.

After calculating the non-dimensional pressure coefficient, the peak values are extracted from the time series at each tap locations by using the approach introduced in Ref. (Sadek and Simiu 2002). Sadek and Simiu (2002) investigated the influence of the time-series duration and sampling frequency on the estimated peaks of input time series. In order to develop the procedure, the appropriate marginal probability distribution of the time series using the probability plot correlation coefficient method was identified and then used to estimate the distribution of the peaks by implementing the standard translation processes approach. They showed that the peaks estimated by the proposed procedure are less dependent than observed peaks on record length and sampling rates.

Accordingly, a MATLAB function for computing of quantiles (i.e., values corresponding to specified probabilities of non-exceedance) of the maximum and minimum values of the input time series was developed which is accessible on the NIST website (Main 2011). This function is used to calculate quantiles of the maximum and minimum values of time series of pressure coefficients.

To make it more tangible, a minimum 95% quantile peak means that the resulting value has a 5% probability of being exceeded in the negative direction for negative peak pressures corresponding to peak suction effects on the roof. For more details, readers are encouraged to check: (Main 2011, Sadek and Simiu 2002).



Fig. 6 Arrangement of passive planks used for adjusting wind velocity profile; (left): front view; (right): lateral elevation

3. Results

3.1 Wind profile measurements and verification

Following the experimental setup and procedure, it was first aimed to figure out how the wind profile could be in the lab by conducting wind speed measurements along the height of the test section at specific along-wind locations by using Cobra probes. In order to properly replicate near-surface ABL wind speed profiles and turbulence intensities within the open-jet facility according to real storm wind conditions, a passive adjustable planks mechanism was used to generate the vertical profile of wind flows in accordance to the desirable target terrain characteristics by changing the pitch angles of planks and using a trial and error procedure. Aly and Chokwitthaya (2014) carried out numerical investigations via Computational Fluid Dynamics (CFD) to reduce the effort required to experimentally create wind profiles that mimic open and suburban terrain within the new open-jet facility at LSU. They also checked wind profiles at cross-section at various locations from exit of open-jet to address the uniformity or skewness of flow across the testing section in the lateral direction. Experimental results showed that the planks arrangement suggested by CFD simulation can create wind speed profiles with desired characteristics. The final plank arrangement can be seen in Fig. 6. Once a certain planks' arrangement was set up based on the CFD results, velocity measurements for 30 seconds were carried out at each point for each location by using a Cobra probe.

Three minutes measurements were also carried out for spectral analysis. The data were analyzed by extracting the mean velocities and turbulence intensities at each measured point to create the corresponding experimental profiles. The mean wind speed profiles resulted from the tests have then been compared with theoretical values by using the power-law exponential wind profile, the logarithmic-law, and the ESDU formulation. The logarithmic-law for the mean wind speed model can be defined by Eq. (3) (Holmes 2015).

$$\bar{U}(z) = \frac{1}{\kappa} u_* \ln \left(\frac{z - z_d}{z_0} \right) = \frac{u_*}{\kappa} [\ln(z - z_d) - \ln z_0] \quad (3)$$

where z denotes the height above surface, z_d is a “zero-plane displacement”, z_0 stands for the roughness length, κ denotes von Kármán constant ($\cong 0.41$), $\bar{U}(z)$ is the mean wind speed at height z , and u_* is the friction velocity. In structural engineering practice, z_d is often considered to be zero.

The power-law mean wind profile is given by Eq. (4) (Holmes 2015).

$$\bar{U}(z) = \bar{U}_{10}(z/10)^\alpha \quad (4)$$

This expression relates the mean wind speed $\bar{U}(z)$ at any given height z above surface to a reference wind speed at 10 m height \bar{U}_{10} ; α is an exponent which depends on the terrain roughness length and height ranges. It can be related as follows in Eq. (5) (Holmes 2015)

$$\alpha = 1 / \ln(z_{ref} / z_0) \quad (5)$$

where z_{ref} is the reference height. In addition to the aforementioned wind profiles, ESDU (ESDU 1982) proposes a wind profile as follows

$$\bar{U}(z) = \frac{u_*}{\kappa} (\ln(z/z_0) + 34.5f z/u_*) \quad (6)$$

in which the Coriolis parameter f is approximated as 10^{-4} Hz.

Fig. 7 shows various locations of the velocity measurements, from the exit of the open-jet (distance d , as a function of the flow height H). Fig. 8(a), presents the measured along-wind mean velocity profiles in center-line of the test section in open-jet at various heights for different distances from the exit of the fans, along with the theoretical profiles by using the power-law, the logarithmic-law, and the ESDU formulations. It can be seen that the measured wind velocity data are consistent with theoretical wind profiles for open-terrain condition characteristics in almost 2/3 of the height of wind field, and after that height the experimental velocity magnitudes are decreasing as the profile is reaching the highest point of test section (α was considered 0.15, and z_0 was selected 0.01 m for open terrain condition according to (Holmes 2015)). The test models were placed in the lower part of the test section, so the lower part of simulated wind profiles in the LSU WISE open-jet facility were well representative of open-terrain conditions around the building models. It should be noted that in theoretical formulations, the wind velocity (U_{ref}) is 15.49 m/s at 3.96 m (roof height in full scale). And for normalizing the experimental results in Fig. 8, $H_{ref} = 26$ cm (~ 10 inch), which is equal to roof height for building model with scale of 1:15; and U_{ref} is the mean of wind velocity measurements at H_{ref} ; (U_{ref} is different for each of the four measurements).

Fig. 8(b), shows the along-wind turbulence intensity profiles at various locations in the open-jet test section. Within Fig. 8(b), two profiles based on $1/\ln(z/z_0)$ formulation and the ESDU equation are presented with the measured experimental data. The intensity of turbulence introduced by ESDU (ESDU 1983) is expressed in Eq. (7)

$$I_u = \frac{\sigma_u}{U_z} \rightarrow \frac{\sigma_u}{u_*} = \frac{7.5\eta[0.538 + 0.09\ln(z/z_0)]^{\eta^{16}}}{1 + 0.156\ln(u_*/(f z_0))} \quad (7)$$

where $\eta = 1 - 6f z/u_*$.

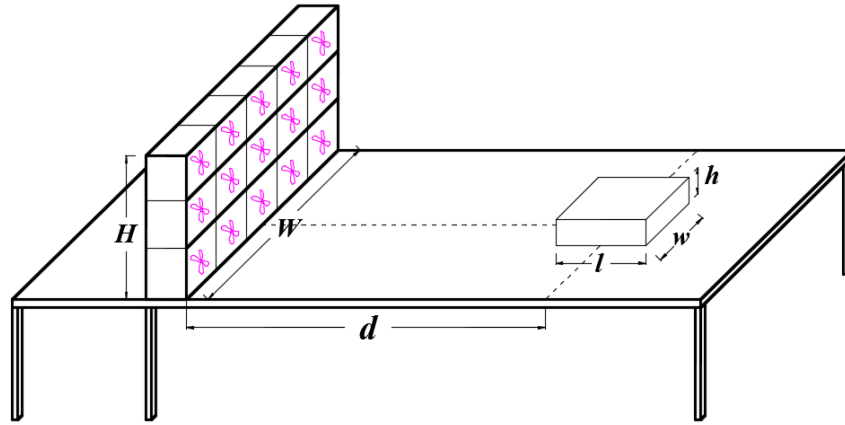


Fig. 7 Various locations were considered in order to investigate the optimal horizontal distance of a test building from the exit of the open-jet facility, ($d=H, 1.5H, 2H, 2.5H$)

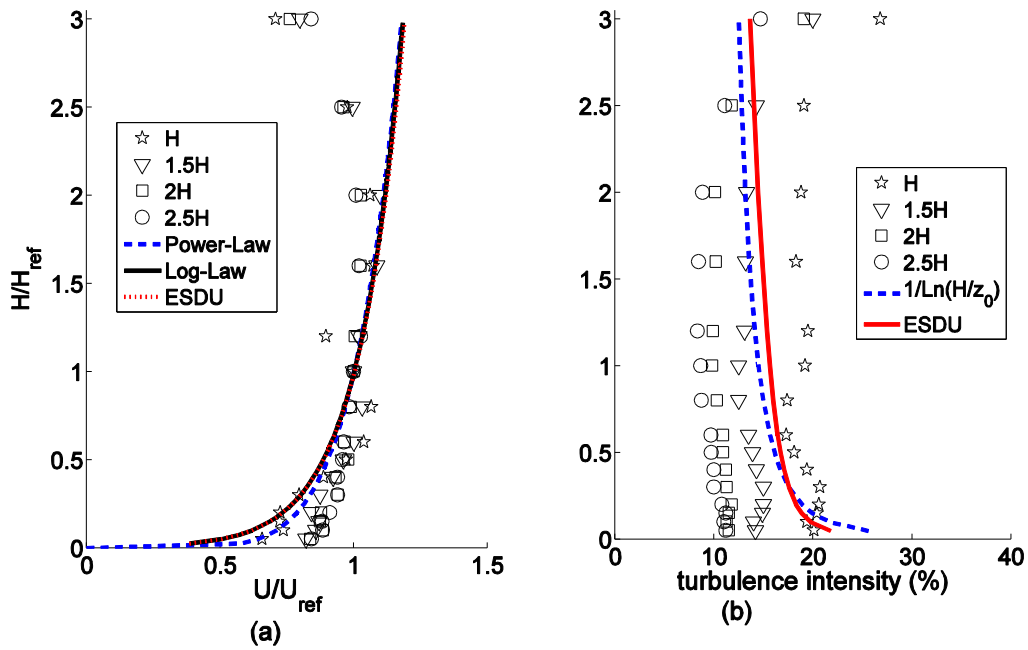


Fig. 8 Laboratory along-wind velocity measurements (a) along-wind normalized mean velocity profiles and (b) along-wind turbulence intensity profiles

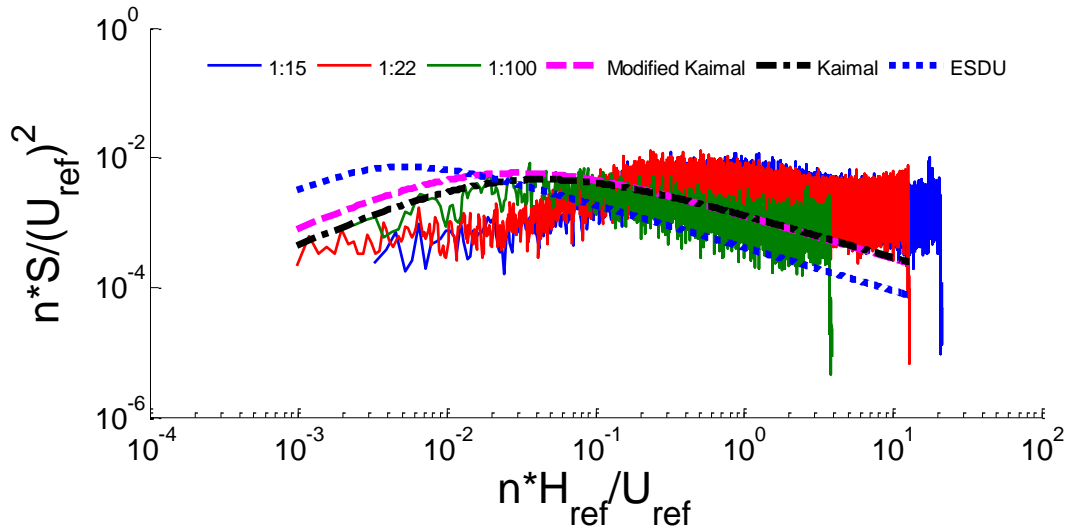


Fig. 9 Along-wind velocity spectra at 2.5H distance converted to full-scale

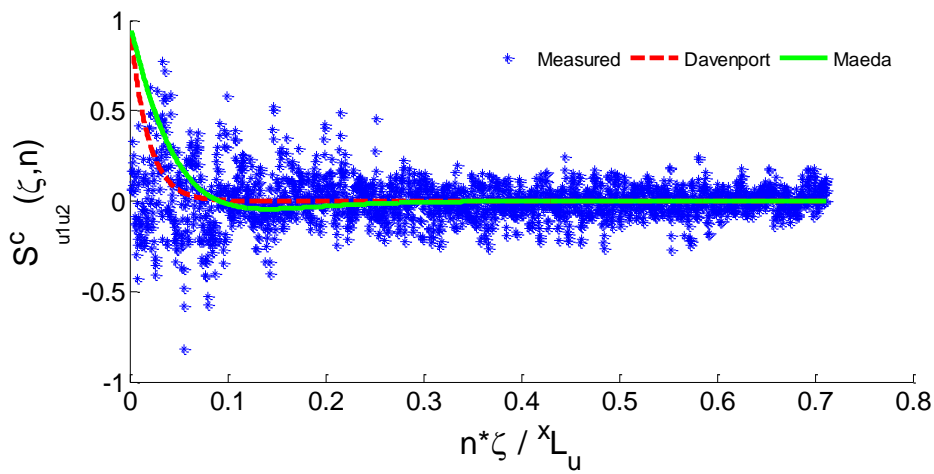


Fig. 10 Non-dimensional cross-spectra of u-component for two vertically-distantly-positioned points of A and B and the theoretical counterparts

According to the results, it is shown that the open-jet facility is able to properly replicate near-surface ABL profiles and turbulence intensities suitable to real conditions of open-terrain. Moreover, as the distance from the exit of open-jet is increasing, the turbulence intensity magnitude is decreasing.

In addition to mean velocity and turbulence intensity profiles, the spectral characteristics of wind flow are very important, especially to simulate fluid-structure interaction and peak aerodynamic

loads. The turbulence structure in a wind flow can be specified by its spectral content. High frequency vortices are responsible for energy dissipation and more importantly the proper formation of the flow patterns around a bluff body (Stathopoulos and Surry 1983). Large eddies in a flow contribute significantly to peak aerodynamic loads. In fact, the generation of turbulence in a flow with a certain spectral content presents a challenge for both experimental and numerical simulations of ABL winds. In Fig. 9, the along-wind velocity spectra for measured velocity data at reference heights is plotted for two scale models at 2.5H distance from the exit of the open-jet (H is the wind field height). The time scale and velocity scale are imposed on the measured data in the lab and the spectra are therefore for the full-scale case. In addition, the Kaimal and the ESDU spectra were calculated according to the theoretical formulations (plotted in Fig. 10).

The Kaimal spectrum is defined as follows (Kaimal *et al.* 1972)

$$\frac{f S_{aa}(f)}{u_*^2} = \frac{An}{(1+Bn)^{5/3}} \quad (8)$$

in which $f \equiv nU/z$. For the along-wind velocity spectrum, S_{uu} may be calculated by considering $A = 105$ and $B = 33$. A modified form of Kaimal spectrum for S_{uu} was proposed where $A = 200$ and $B = 50$ (Simiu 2011, Simiu and Scanlan 1996). In order to quantify the vertical velocity fluctuations, S_{vv} , up to an elevation of about 50 m, the formula in Eq. (8) can be used by considering: $A = 3.36$, and $B = 10$ (Simiu, 2011, Simiu and Scanlan 1996); a similar way can be adopted for the lateral turbulent fluctuations, S_{ww} , by considering: $A = 15$, and $B = 9.5$ (Simiu and Scanlan 1996). The ESDU spectrum is proposed based on new von Karman spectrum for the complete frequency range as follows (ESDU 2001):

$$\frac{f S_{uu}(f)}{\sigma_u^2} = \beta_1 \frac{2.987n_u/\alpha}{[1+(2\pi n_u/\alpha)^2]^{5/6}} + \beta_2 \frac{1.294n_u/\alpha}{[1+(\pi n_u/\alpha)^2]^{5/6}} F_1. \quad (9)$$

For more details regarding the ESDU spectrum and definition of different terms, readers are referred to Ref. (ESDU 2001). The non-dimensional cross-spectrum of the fluctuating along-wind velocity component (u-component) for two vertically-distantly-positioned points of A and B is defined as follows (Fujimura and Maeda 2009)

$$\tilde{S}_u^c(\zeta, n) = \frac{S_u^c(\zeta, n)}{\sqrt{S_{uA}(n)}\sqrt{S_{uB}(n)}}, \quad (10)$$

$$S_u^c(\zeta, n) = \int_{-\infty}^{\infty} R_u^c(\zeta, \tau) \exp(-j2\pi n\tau) d\tau. \quad (11)$$

where $R_u^c(\zeta, \tau) = E[u_A(t)u_B(t+\tau)]$, $S_{uA}(n)$ and $S_{uB}(n)$ are the power spectra at points A and B respectively, ζ is the vertical distance between points A and B, and n is the frequency. The non-dimensional cross-spectrum of Davenport and an approximate expression of the Karman type proposed by (Maeda and Makino 1980) are as follows

Davenport

$$\tilde{S}_u^c(\zeta, n) = \exp\left(-k_r \frac{|n\zeta|}{U}\right), \quad (12)$$

$$\text{Maeda and Makino: } \tilde{S}_u^c(\zeta, n) = \exp(-k_1\theta)(1 - k_2\theta^2), \quad (13)$$

where $k_r = 13(\zeta/z_m)^{0.4}$, $z_m = 0.5(z_A + z_B)$, $\theta = \left\{ (0.747\zeta/xL_u)^2 + (2\pi n\zeta/\bar{U})^2 \right\}^{1/2}$, $k_1 = 1.0$, and $k_2 = 0.2$ (Fujimura and Maeda 2009).

According to Fig. 9, it is shown that the open-jet facility is able to simulate large eddies in the flow. In fact, this capability contributes significantly for the prediction of peak aerodynamic loads over the surface of building models, especially on the edges of roofs that are the most vulnerable parts of low-rise buildings under the suction effects induced by hurricane winds. However, according to Fig. 9, there is a substantial difference between the ESDU spectrum contents compared with Kaimal and the modified Kaimal. This discrepancy was also reported in (Mann 2012, Mann *et al.* 1998). It is believed to be due to the larger along-wind velocity length scales assumed by ESDU which was supported by (Højstrup *et al.* 1990). Fig. 10 shows the non-dimensional cross-spectra of u-component for 2 vertically-distantly-positioned points at $d=2.5H$ from the exit of the open-jet facility ($z_A = 4\text{m}$ corresponding to roof height and $z_B = 0.89\text{m}$, both in full scale).

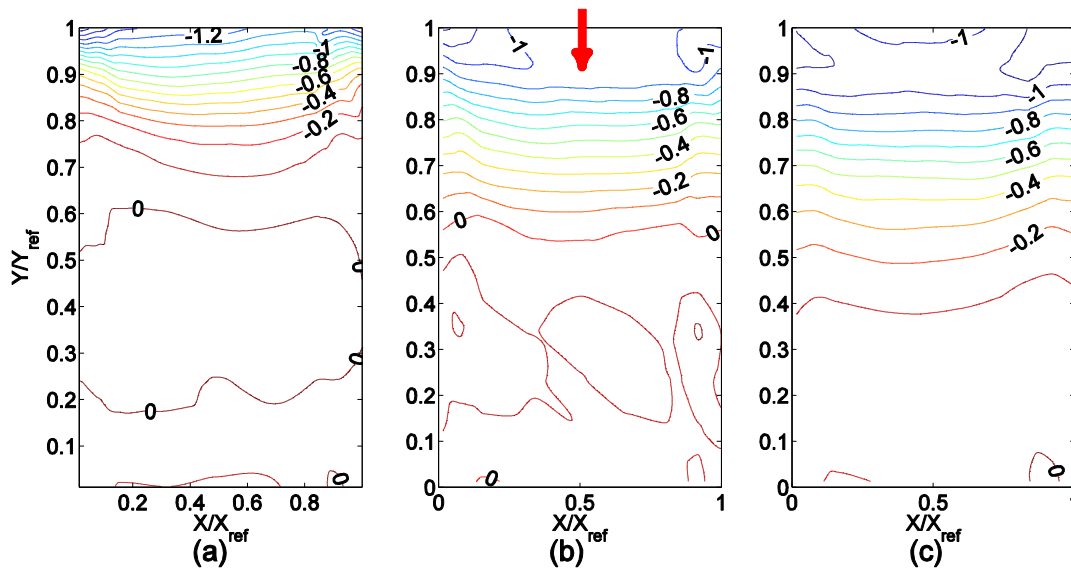


Fig. 11 LSU mean roof CPs at $\phi = 0^\circ$, scale 1:22: (a) at distance of $1H$ from the exit of the open-jet, (b) at a distance of $1.5H$ and (c) at a distance of $2H$

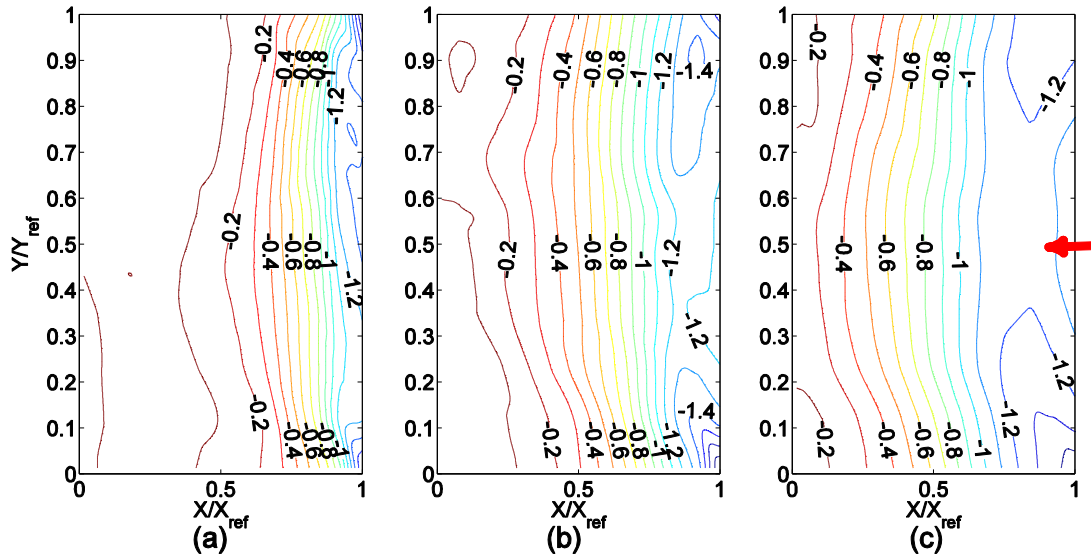


Fig. 12 LSU mean roof CPs at $\phi = 90^\circ$, scale 1:22: (a) at a distance $d = 1H$, (b) $d = 1.5H$ and (c) $d = 2H$

3.2 Determination of optimal distance

As described earlier, one important target in this research is to determine the optimal distance of a test building from the exit of the open-jet facility by means of conducting several investigations on two small scale models. Fig. 7 shows the various locations of the models from the exit of the open-jet facility on the centerline of the test section. At each location, tests were carried out for 0° and 90° direction angles. Fig. 11 shows the contours of mean pressure coefficients for LSU 1:22 scale model at various locations of $d=H$, $1.5H$, $2H$ from the exit of the open-jet simulator at a wind direction angle of 0° ($X_{ref} = 0.41$ m, and $Y_{ref} = 0.61$ m). In all cases, it is shown that the non-dimensional wind pressure coefficients are negative in most parts of the roof, meaning that the roof is almost under the suction effect. However, the pattern of wind pressure coefficients is changing as the model is placed in a far distance from the exit of open-jet. For instance, in Fig. 11(a) at $d = H$, within the $2/3$ of roof area, the values of mean pressure coefficients are around zero, while in Fig. 11(c) at $d = 2H$ within around $1/3$ of roof area, the mean pressure coefficients are around zero. This reveals an important conclusion that the flow pattern over the surface of the roof is sensitive to its location from the exit of the open-jet. The separation bubble is shorter for models located closer to the exit of the open-jet. This may be attributed to the higher turbulence intensity associated with the model proximity (Fig. 8(b)). The higher turbulence intensity is contributed by high frequency turbulence (small scale turbulence), as will be discussed later in Section 4. It could also mean that test models located closer to the exit of the open-jet are subjected to more blockage than those located further downstream. For all locations, the flow reattachment is significant for this test scenario that has $l/h = 3.46$: l is the roof along-wind dimension, and h is the roof height.

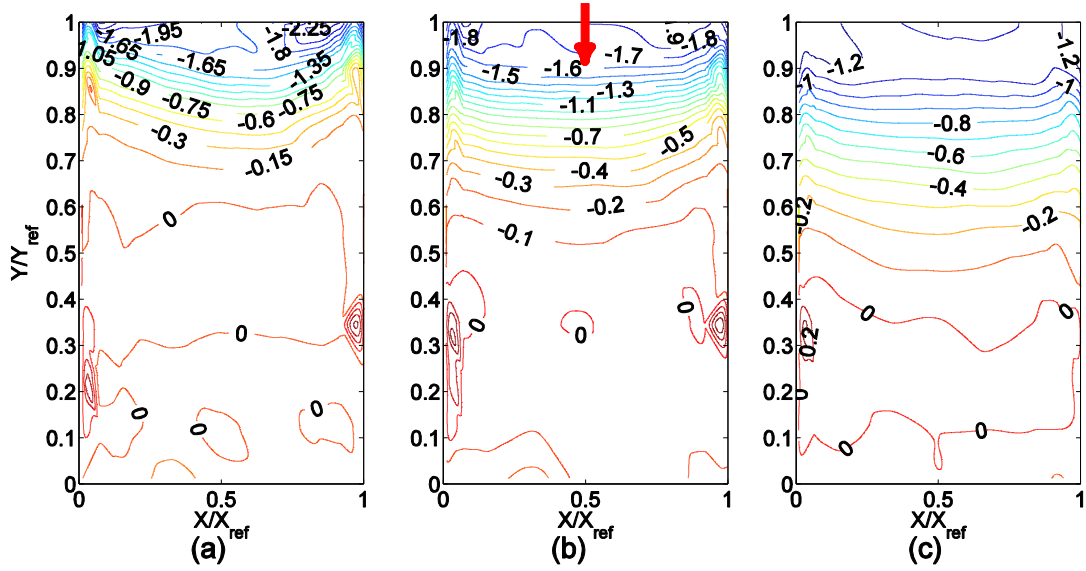


Fig. 13 LSU mean roof CPs at $\phi = 0^\circ$, scale 1:15: (a) $d = 1H$, (b) $d = 1.5H$ and (c) $d = 2H$

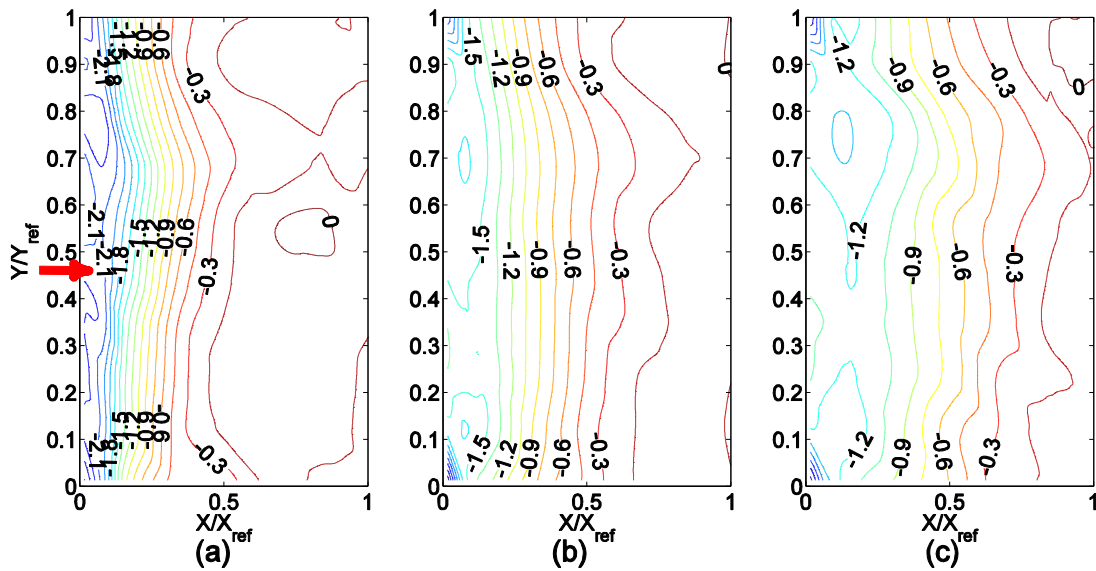


Fig. 14 LSU mean roof CPs for $\phi = 270^\circ$, scale 1:15: (a) at $d = 1H$, (b) $d = 1.5H$ and (c) $d = 2H$

Fig. 12 shows contours of mean pressure coefficients for a roof of a test model scaled 1:22 at 90° for three different locations from the exit of the open-jet: 1H, 1.5H and 2H. Although a similar trend to Fig. 11 can be seen in contours of wind pressure coefficients in Fig. 12, there is still a difference in flow reattachment pattern which is mainly affected by the shorter dimension of roof in the along-wind direction when the tests are carried out at 90° direction angle ($l/h = 2.30$).

Figs. 13 and 14 show the contours of mean pressure coefficients for a model scaled 1:15 at various locations of $d=H$, 1.5H, 2H from the exit of the open-jet facility at 0° and 270° direction angles. In these plots X_{ref} is 0.61 m and Y_{ref} is 0.91 m. Again as shown in the 1:22 scale, closer the test model to the open-jet exit, shorter the separation bubble.

Fig. 15 represents the minimum 95% quantile peak pressure coefficients for the LSU 1:15 scale model at various distances from the exit of the open-jet facility. It is seen that as the distance from the exit of open-jet is decreasing, the values of peak CPs are increasing within the shorter edges of roof in windward. For instance, Fig. 15(a), the values of minimum 95% quantile peak pressure coefficients are reaching to a value around -10 in some spots which is a huge difference from the peak value in Fig. 15(c) which is around -3.6. It is due to the fact that at distance of $d=1H$ from the exit of open-jet, turbulence intensity magnitude is much higher, and also high frequency turbulence in approaching flow contribute significantly to those peak aerodynamic loads (this will be further discussed in Section 4). Therefore, it is crucial to consider the optimal distance from the exit of the open-jet in order to avoid recording overestimated values of peak pressures in the lab. This aim was satisfied by conducting tests at $d=2.5H$ and the results will be presented in the following subsection.

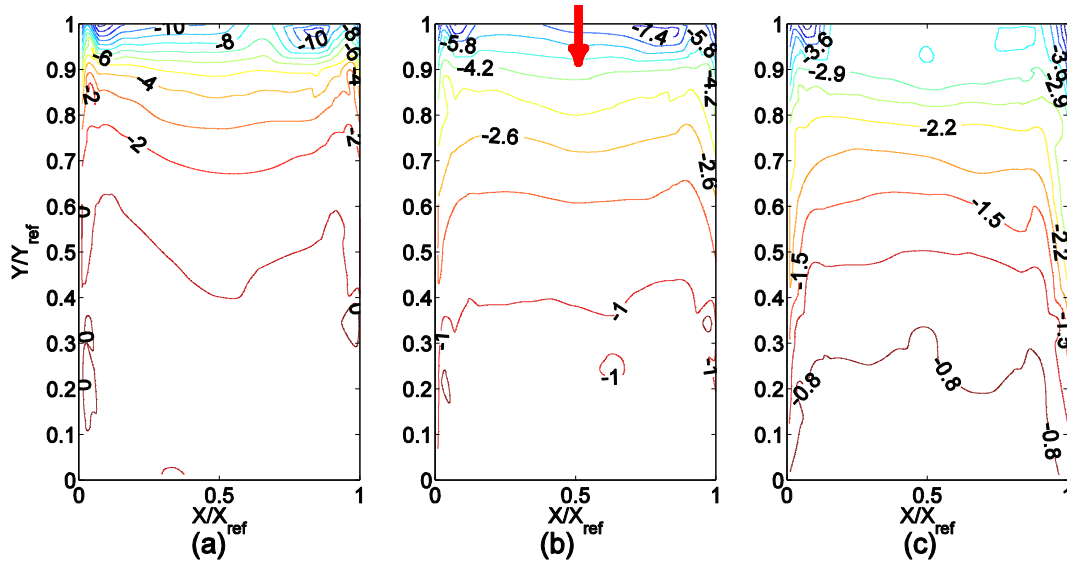


Fig. 15 Minimum 95% quantile peak CPs for $\phi = 0^\circ$, scale 1:15: (a) at $d = 1H$, (b) $d = 1.5H$ and (c) $d = 2H$

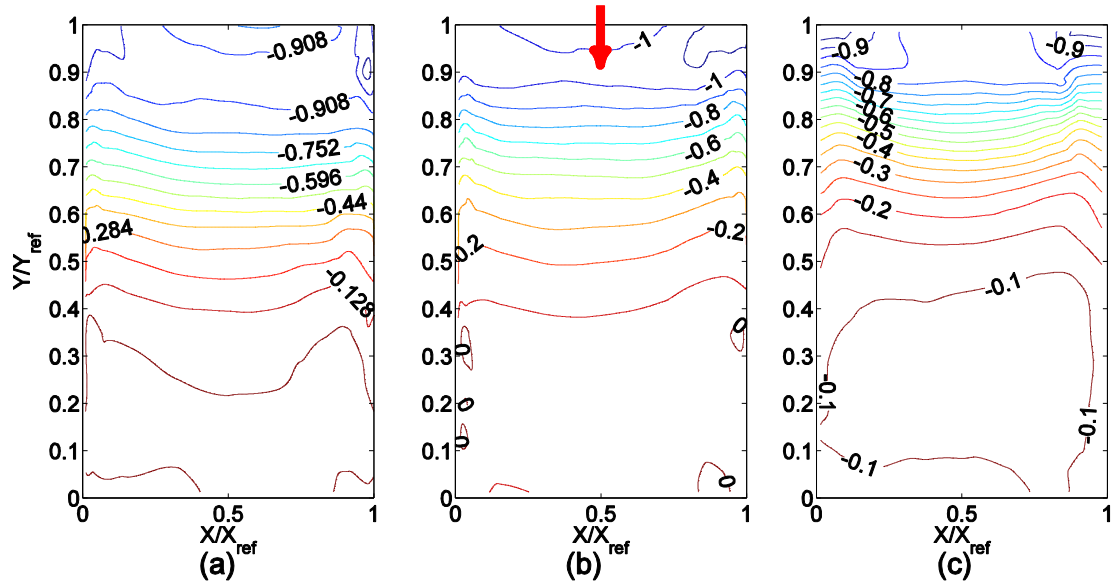


Fig. 16 Mean roof CPs at a distance of 2.5H from the exit of the open-jet for $\phi = 0^\circ$; (a) LSU at scale 1:15, (b) LSU at scale 1:22 and (c) NIST at scale 1:100

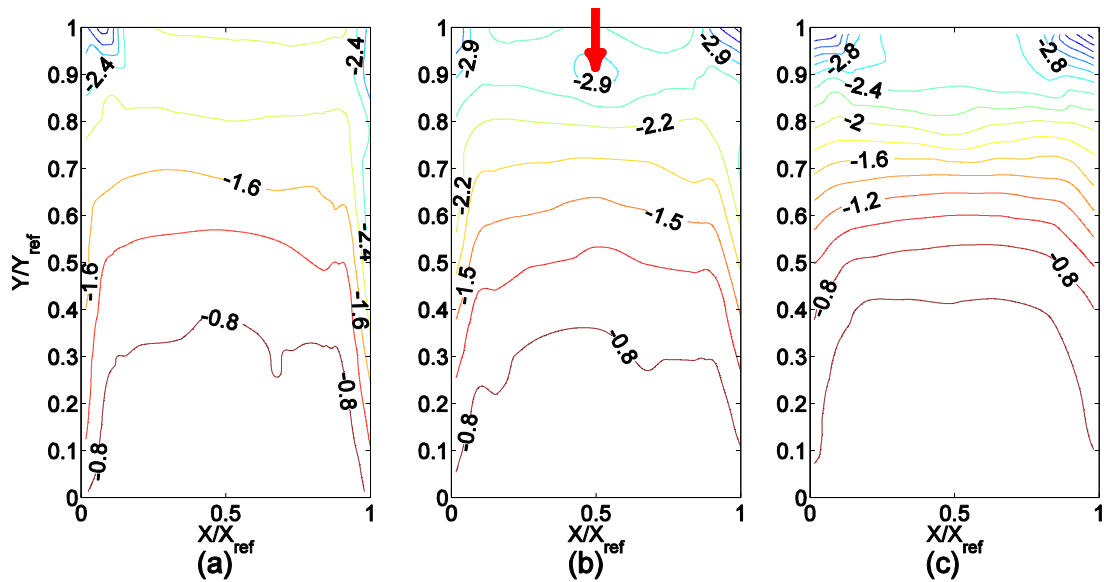


Fig. 17 Minimum 50% quantile peak roof CPs at a distance of 2.5H from the exit of the open-jet for $\phi = 0^\circ$; (a) LSU at scale 1:15, (b) LSU at scale 1:22 and (c) NIST at scale 1:100

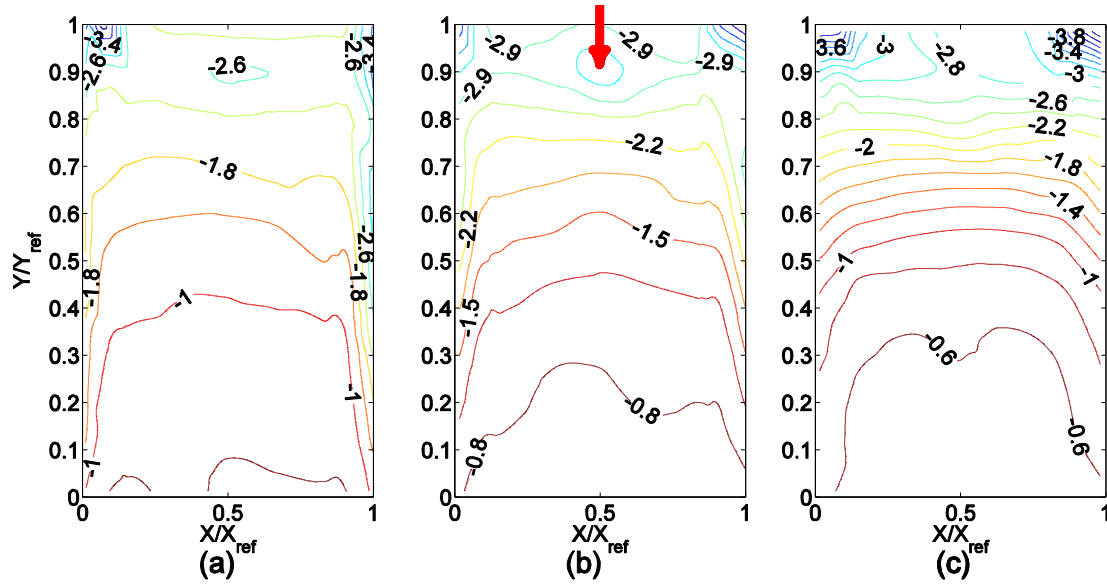


Fig. 18 Minimum 95% quantile peak roof CPs at a distance of $2.5H$ from the exit of the open-jet for $\phi = 0^\circ$; (a) LSU at scale 1:15, (b) LSU at scale 1:22 and (c) NIST at scale 1:100

3.3 Effects of model scale on pressure distribution

The scale effect on the wind pressure distributions was investigated by testing two models of the low-rise building in the open-jet facility and comparing the results with a benchmark 1:100 scale model from NIST/UWO database wind tunnel testing. The aim is to know what scale is more suitable for testing in the LSU WISE open-jet facility in order to produce reliable results with acceptable resolution for wind pressure coefficients over the roofs of buildings.

Figs. 16-18 represent contours of mean, minimum 50% quantile peak, and minimum 95% quantile peak pressure coefficients for the two LSU scale models at $d=2.5H$ from the exit of open-jet facility, and the same contours for the NIST 1:100 scaled model at 0° direction angle. According to Fig. 16, although the values of mean pressure coefficients on the two LSU scale models are pretty well matched with the results of the NIST model, it seems that the pattern of the pressure contours for the 1:15 model is a better representative for mean values.

Figs. 17 and 18 show that reliable peak values of pressure distribution are achieved by testing a 1:15 scale model. This means that a test model with $0.3H$ (height) \times $0.36W$ (width) \times $1H$ (length) can be tested at $2.5H$ distance from the open-jet facility to provide reliable mean and peak pressure coefficients: 'H' and 'W' are height and width of the open-jet at its exit, respectively.

Figs. 19-21 show contours of mean, minimum 50% quantile peak, and minimum 95% quantile peak pressure coefficients for the two LSU scale models at $d=2.5H$ from the exit of the open-jet facility, along with results from the NIST 1:100 scale model at 90° . According to Fig. 19, a similar conclusion to Fig. 16 can be drawn for mean pressure coefficients. In these cases, the model with scale 1:15 can be introduced as the best match with NIST mean pressure coefficient results.

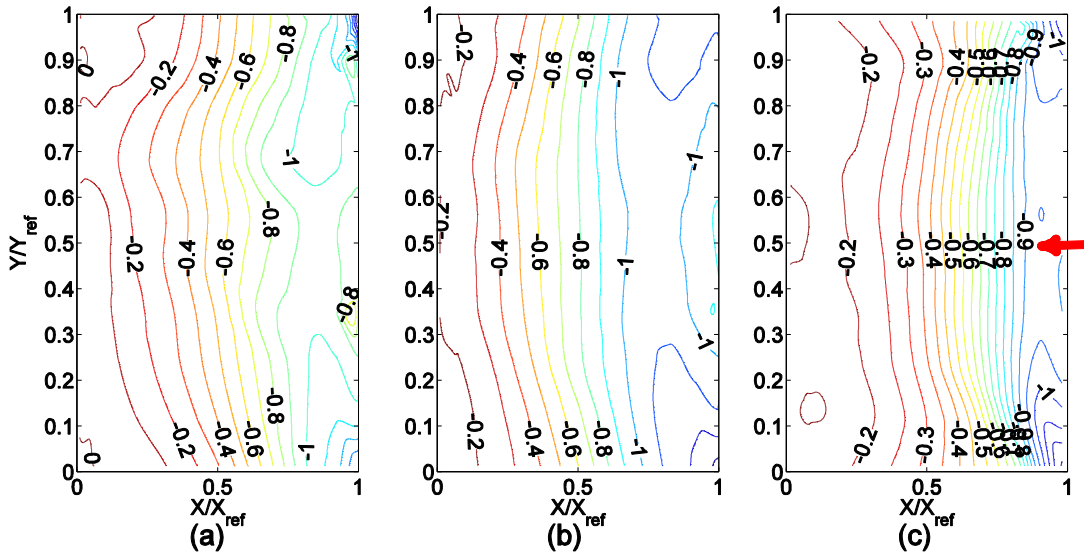


Fig. 19 Mean roof CPs at a distance of 2.5H from the exit of the open-jet for $\phi = 90^\circ$; (a) LSU at scale 1:15, (b) LSU at scale 1:22 and (c) NIST at scale 1:100

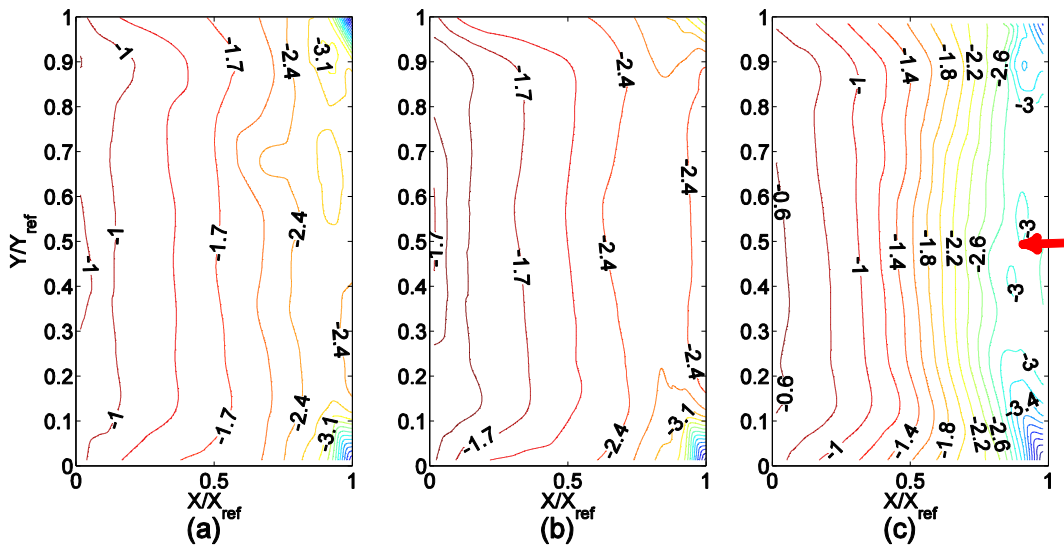


Fig. 20 Minimum 50% quantile peak roof CPs at a distance of 2.5H from the exit of the open-jet for $\phi = 90^\circ$; (a) LSU at scale 1:15, (b) LSU at scale 1:22 and (c) NIST at scale 1:100

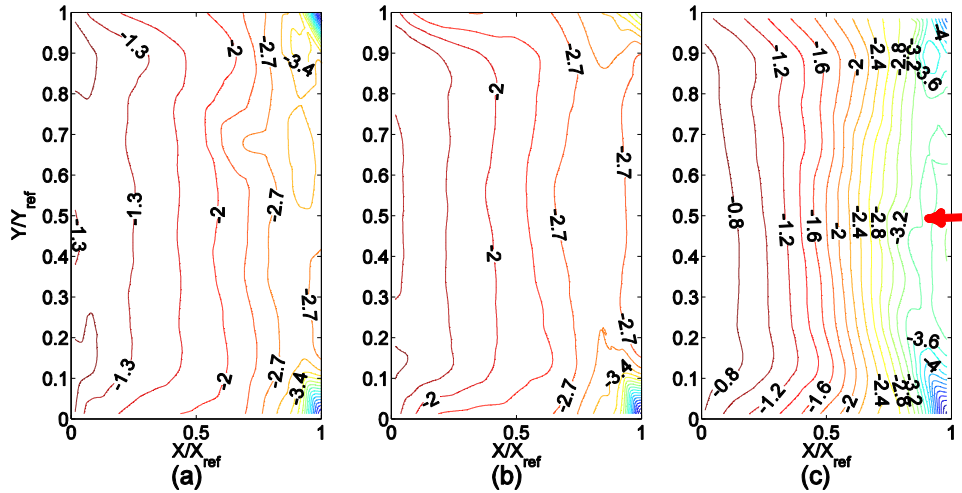


Fig. 21 Minimum 95% quantile peak roof CPs at a distance of $2.5H$ from the exit of the open-jet for $\phi = 90^\circ$; (a) LSU at scale 1:15; (b) LSU at scale 1:22; and (c) NIST at scale 1:100

Also, by comparing the results of peak pressure coefficients in Figs. 20 and 21, it can be concluded that a test model at $d=2.5H$ is a good representative of the test scenario introduced by NIST. For this wind direction angle (90°), it means that a test model with $0.3H$ (height) \times $0.54W$ (width) \times $0.67H$ (length) can be tested at $2.5H$ distance from the open-jet facility to provide reliable mean and peak pressure coefficients: 'H' and 'W' are height and width of the open-jet at its exit, respectively.

By combining all results achieved in this study it can be concluded that: (i) the optimal location for testing at the open-jet facility is at a distance two times and half the wind field at its exit, (ii) the optimal width of a test building is half the width of the wind field, and (iii) the optimal length of the test model is same as the wind field height at its exit from the facility.

4. Discussion

The results of mean pressures presented above show dependence of the flow pattern (length of the separation bubble) on the roof of the test building on the location from the exit of the open-jet. Mean pressure distribution was distinguishable among models tested with different proximity to the flow source. While open-jet blockage could be the issue that is models tested closer to the jet exit have more blockage than those tested further downstream, turbulence structure may have the most influential effects. As noticed early in Fig. 8(b), the turbulence intensity is higher closer to the exit of the jet. However, the reason for having different mean pressure patterns seems to be attributed to the flow structure, rather than just the turbulence intensity in its general meaning. To further investigate this issue, Fig. 22 shows the spectral content of the along-wind velocity component at different locations from the exit of the open-jet ($1H$, $1.5H$, $2H$, and $2.5H$) at height of 3.9 cm corresponding to 1:100 scaled down roof height of 3.96 m in full-scale. The spectrum is normalized with respect to U_{ref}^2 similar to Davenport (1961).

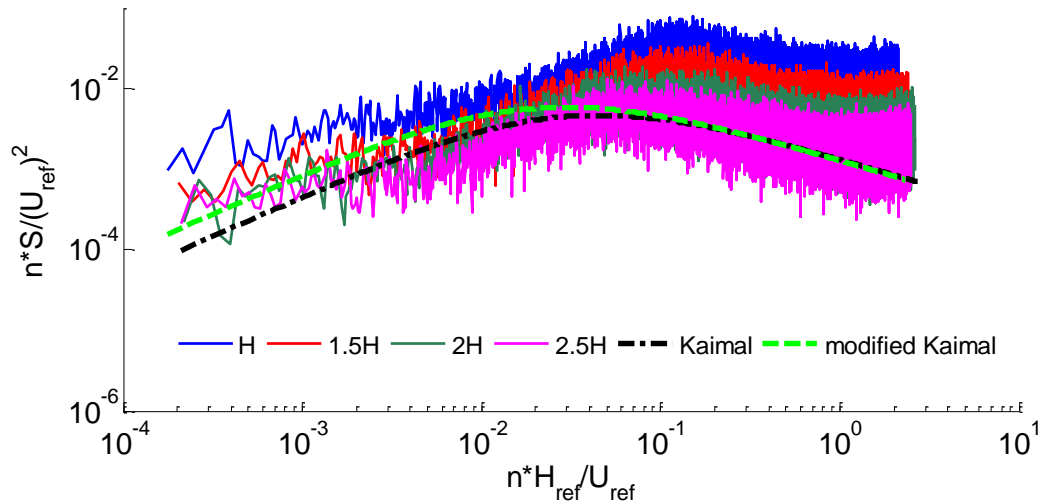


Fig. 22 Along-wind velocity spectra at various distances of 1H, 1.5H, 2H, and 2.5H from the exit of open-jet simulator

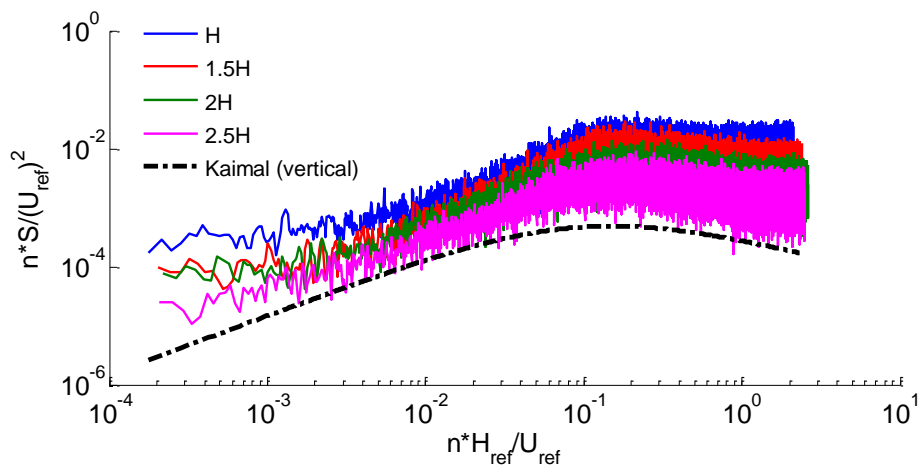


Fig. 23 Velocity spectra for vertical direction wind fluctuations at various distances of 1H, 1.5H, 2H, and 2.5H from the exit of open-jet simulator

In addition, Figs. 23 and 24 show the velocity spectra for vertical and lateral direction wind fluctuations along with the theoretical Kaimal spectra. It is shown that the measured spectrum for the along-wind velocity component and also the lateral velocity component are well matched with the counterpart theoretical Kaimal spectrum at 2.5H. The velocity spectrum for the vertical direction shows higher energy and turbulence level in all frequency ranges in compare to the theoretical Kaimal spectrum even at 2.5H. However, the pattern and distribution of energy in all frequency

ranges are similar. This mismatch may be improved by developing additional active turbulence generation mechanisms for simulating appropriate turbulence spectrum matching the target spectrum in vertical direction. It is a subject of undergoing investigations at the LSU WISE research program to improve the capability of the constructed open-jet facility.

It is known that a real flow structure in nature consists of low-frequency and high-frequency eddies (Sagaut 2006). By looking at Figs. 22-24, it is noticeable that in all cases, the turbulence structure changes as the flow moves further downstream, especially the high-frequency content. Although the turbulence in all frequency range increases as the test location get close to the jet exit, it is shown that closer the test location to the exit of the open-jet, higher the small scale turbulence. It is believed that the flow pattern around a bluff-body are sensitive to the high-frequency turbulence (small eddies in the flow) (Tieleman *et al.* 1996), which is valid in recent studies (Aly 2016, 2014, Aly and Bitsuamlak 2013).

The presence of high-frequency turbulence at close proximity to the open-jet is attributed to the small eddies produced by the fans and flow separation over the planks and the wooden frame. Such eddies are eliminated at further distance downstream due to energy dissipation (Kolmogorov 1941). It is warranted to pay attention for not testing at a close proximity to the exit of an open-jet facility, especially buildings with roof top equipment, for instance solar panels, and metal roofing as this may lead to overestimated wind loads in the separation bubble, associated with unrealistic vibrations. In all testing scenarios, the high frequency part of the wind velocity spectrum should not be much higher than the counterpart target test flow.

Peak pressures on the roof are very sensitive to the turbulence structure. While the spectral content showed strong influence on the separation bubble length, high frequency turbulence in the flow is responsible for excessive fluctuations within the separation bubble. Fluctuations close to the leading edge of the test models are much higher than typical values expected in wind tunnels, when the test object is located close to the exit of the open-jet. This is very important as destructive testing of buildings may be carried out closer to the exit of the jet to experience flow at high speed.

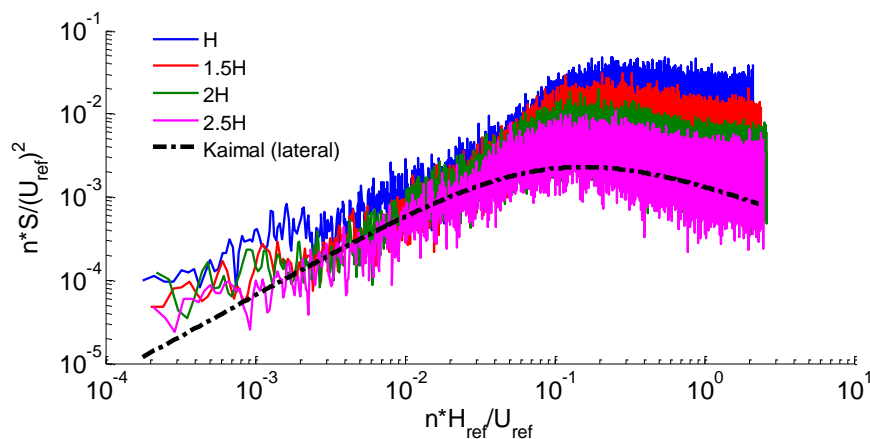


Fig. 24 Velocity spectra for lateral direction wind fluctuations at various distances of 1H, 1.5H, 2H, and 2.5H from the exit of open-jet simulator

In such case, pressure fluctuations may not be a true representative of the full-scale flow counterpart. The sensitivity of wind loads on buildings to flow conditions makes bluff body aerodynamics an everlasting challenge. In fact such sensitivity is a reason for discrepancies among results obtained from different laboratory testing (Fritz *et al.* 2008). This argue the need for a standardized testing protocols to eliminate/reduce discrepancies in wind engineering testing. Future research should focus on such protocols as well as promising computational methods, such as, CFD (Blocken 2014, Blocken *et al.* 2007).

The current study enabled testing 1:15 scale model with comparable results to those obtained by testing at 1:100 in a wind tunnel. Consequently, large test models can be tested at the open-jet facility with no blockage issues. The corresponding wind tunnel blockage for such model is 16% (the ratio of the frontal area of the model to the area at inlet occupied by fans) that could cause issues with pressure distribution if the same size was tested in a wind tunnel with same flow cross-section area. It is worthy to mention that the maximum allowable blockage in wind tunnels is about 5% (Holmes 2015). Any deviation from this blockage limit in wind tunnel testing usually requires corrections of collected pressure data. This indicates the capability of the open-jet facility to achieve reliable mean and peak pressures on large size test models without significant blockage or scale issues.

Last but not least, the results and findings of this study can be extended and used for proposing guidelines on conducting test scenarios in open-jet facilities, eventually helping the development of improved standard provisions on wind effects on low-rise buildings. The concept of ABL simulation in small scale open-jet facility as elaborated in this paper can be extended to large-scale testing facilities capable of generating sustained hurricane wind in companion with wave simulation facilities to allow a better understanding of extreme winds and their effects on offshore and onshore infrastructures. Such comprehensive large-scale models of built environment will help to improve environmental sustainability, mitigate the devastating effects of extreme winds, and produce solutions which bridge the disciplines of atmospheric sciences, wind engineering and structural engineering.

5. Conclusions

In this paper, the challenges involved in the appropriate simulation of near-surface atmospheric boundary-layer wind characteristics for buildings at the newly constructed LSU WISE open-jet facility are addressed. Experimental studies on two small-scale building models were carried out and the results are compared with available wind tunnel data from NIST/UWO. The main contributions of this study are summarized as follows:

- The mean velocity profile can be simulated in the LSU WISE open-jet facility in accordance to near-surface ABL theoretical profiles for the open-terrain condition. However, the turbulence intensity profile and the power spectrum of the along-wind velocity are sensitive to the proximity to the exit of the open-jet. Closer the test location to the exit of the open-jet, higher the small scale turbulence.
- Mean values of pressure coefficients are correlated with the location of the test model from the exit of the open-jet. Closer the test model to the exit of the open-jet, shorter the separation bubble.
- Peak pressures in the separation bubble are highly sensitive to the open-jet exit proximity. This is because small scale turbulence is present at relatively high levels close to the exit of the open-jet. This reveals that the turbulence characteristics of the approaching flow,

specifically high-frequency content, can significantly influence the magnitude of fluctuating pressures.

- For the scale models that are placed at a horizontal distance of $2.5H$ from the exit of the open-jet (H is the height of the wind field), the contours of mean and peak pressure coefficients are consistent with the results of NIST/UWO. This good agreement can be seen in both LSU scale models (1:15 and 1:22).
- The 1:15 scale model is believed to be a better representative of aerodynamic characteristics of the target building based on the comparison of wind-induced mean and peak pressure coefficients measured in the open-jet facility with those from the NIST/UWO results. Consequently, it can be concluded that the optimal width of a test building is half the width of the wind field, and the optimal length of the test model is same as the wind field height at its exit from the facility.
- Testing models with as large as 16% blockage ratio is feasible at the LSU WISE open-jet facility, which is a challenge in wind tunnels. This reveals the importance of open-jet facilities as a promising and robust tool to alleviate the scale restrictions involved in the physical investigation of flow pattern around civil engineering structures.
- The results and findings of this study can be extended and used for putting guidelines for testing protocols at open-jet facilities, eventually helping the development of improved standard provisions on wind effects on low-rise buildings.

Acknowledgements

Financial support from the Louisiana Board of Regents (BoR) was received (Research Competitiveness Subprogram [RCS] and Enhancement Subprogram). Financial support was received from the National Science Foundation (NSF Award No. 1361908), to attend a Planning Grant meeting (IUCRC for Windstorm Hazard Mitigation), and to present the results of this study. The LSU WISE open-jet testing facility would not be built and run without the generous financial support from the following sources: the LSU Office of Research & Economic Development (ORED), NSF through the Louisiana Board of Regents Support Fund (contract no. LEQSF-EPS(2014)-PFUND-345); and the Louisiana Transportation Research Center (LTRC) (project no. 14-2TIRE). The authors would like to thank Joseph Browser and other students who helped assemble the open-jet facility. The physical models of buildings were created partly by assistance of volunteer undergraduate student, Mark Jolissaint.

Disclaimer

The opinions expressed in this paper are those of the authors and do not necessarily reflect the views of any institution/firm.

References

- Aly, A.M. (2014), "Atmospheric boundary-layer simulation for the built environment: Past, present and future", *Build. Environ.*, **75**, 206-221. doi:10.1016/j.buildenv.2014.02.004

- Aly, A.M. (2016), "On the evaluation of wind loads on solar panels: The scale issue", *Sol. Energy*, **135**, 423-434. doi:10.1016/j.solener.2016.06.018
- Aly, A.M. and Bitsuamlak, G. (2013), "Aerodynamics of ground-mounted solar panels: Test model scale effects", *J. Wind Eng. Ind. Aerod.*, **123**, 250-260. doi:10.1016/j.jweia.2013.07.007
- Aly, A.M. and Chokwitthaya, C. (2014), "Atmospheric boundary layer simulation in a new open-jet facility at LSU: CFD and experimental investigations", *Advances in Civil, Environmental, and Materials Research (ACEM14)*, Busan, Korea, August.
- Aly, A.M. and Gol-Zaroudi, H. (2017), "Atmospheric boundary layer simulation in a new open-jet facility at LSU: CFD and experimental investigations", *Measurement*, **110**, 121-133.
- Aly, A.M., Chowdhury, A.G. and Bitsuamlak, G.T. (2011), "Wind profile management and blockage assessment for a new 12-fan wall of wind facility at FIU", *Wind Struct.*, **14**(4), 285-300.
- Aly, A.M., Chowdhury, A.G. and Erwin, J. (2013), "Design and fabrication of a new open jet electric-fan wall of wind facility for coastal research", *Coast. Hazards - Sel. Pap. from EMI 2010*. <https://doi.org/10.1061/9780784412664.014>
- Blocken, B. (2014), "50 years of computational wind engineering: Past, present and future", *J. Wind Eng. Ind. Aerod.*, **129**, 69-102. doi:10.1016/j.jweia.2014.03.008
- Blocken, B., Stathopoulos, T. and Carmeliet, J. (2007), "CFD simulation of the atmospheric boundary layer: wall function problems", *Atmos. Environ.*, **41**, 238-252. doi:10.1016/j.atmosenv.2006.08.019
- Cochran, L. and Derickson, R. (2011), "A physical modeler's view of computational wind engineering", *J. Wind Eng. Ind. Aerod.*, **99**, 139-153. doi:10.1016/j.jweia.2011.01.015
- Davenport, A.G. (1961), "The spectrum of horizontal gustiness near the ground in high winds", *Q. J. R. Meteorol. Soc.*, **87**, 194-211.
- ESDU. (1982), Characteristics of wind speed in the lower layers of the atmosphere near the ground: strong winds (neutral atmosphere). *Eng. Sci. Data Unit, Data Items*.
- ESDU. (1983), Strong Winds in the Atmospheric Boundary Layer. Part 2: Discrete Gust Speeds. *Eng. Sci. Data Unit, Data Items* 108.
- ESDU. (2001), Characteristics of atmospheric turbulence near the ground. Part II: single point data for strong winds (neutral atmosphere). *Eng. Sci. Data Unit, Data Items*.
- Fritz, W.P., Bienkiewicz, B., Cui, B., Flamand, O., Ho, T.C.E., Kikitsu, H., Letchford, C.W. and Simiu, E. (2008), "International Comparison of Wind Tunnel Estimates of Wind Effects on Low-Rise Buildings: Test-Related Uncertainties", *J. Struct. Eng.*, **134**, 1887-1890. doi:10.1061/(ASCE)0733-9445(2008)134:12(1887)
- Fujimura, M. and Maeda, J. (2009), "Cross-correlation of fluctuating components of wind speed based on strong wind measurement", *Proceedings of the 7th Asia-Pacific Conference on Wind Engineering*, T1-D, Taipei.
- Hagos, A., Habte, F., Chowdhury, A.G. and Yeo, D. (2014), "Comparisons of two wind tunnel pressure databases and partial validation against full-scale measurements", *J. Struct. Eng. (United States)*, **140**. doi:10.1061/(ASCE)ST.1943-541X.0001001
- Ho, T.C.E., Surry, D. and Morrish, D.P. (2003), NIST/TTU cooperative agreement--windstorm mitigation initiative: Wind tunnel experiments on generic low buildings. *BLWT-SS20-2003*, Boundary-layer Wind Tunnel Laboratory, Univ. of Western Ontario, London, Canada.
- Højstrup, J., Larsen, S.E. and Madsen, P.H. (1990), "Power spectra of horizontal wind components in the neutral atmospheric surface boundary layer", *Proceedings of the AMS 9th Symposium on Turbulence and Diffusion*, Roskilde, Denmark.
- Holmes, J.D. (2015), *Wind loading of structures*, 3rd Ed., New York: Taylor and Francis.
- Huang, P., Chowdhury, A.G., Bitsuamlak, G. and Liu, R. (2009), "Development of devices and methods for simulation of hurricane winds in a full-scale testing facility", *Wind Struct.*, **12**(2), 151-177.
- Kaimal, J.C.J., Wyngaard, J.C.J., Izumi, Y., Coté, O.R. and Cote, O.R. (1972), "Spectral characteristics of surface-layer turbulence", *Q. J. Meteor. Soc.*, **98**(417), 563-589. doi:10.1002/qj.49709841707
- Knutson, T.R., McBride, J.L., Chan, J., Emanuel, K., Holland, G., Landsea, C., Held, I., Kossin, J.P., Srivastava, A.K. and Sugi, M. (2010), "Tropical cyclones and climate change", *Nat. Geosci.*, **3**, 157-163.
- Kolmogorov, A.N. (1941), "The local structure of turbulence in incompressible viscous fluid for very large

- Reynolds numbers”, *Dokl. Akad. Nauk SSSR*, **30**, 301-305. doi:10.1098/rspa.1991.0075
- Maeda, J. and Makino, M. (1980), “Classification of customary proposed equations related to the component of the mean wind direction in the structure of atmospheric turbulence and these fundamental properties”, *Trans. Archit. Inst. Japan*, 77-87.
- Main, J.A. (2011), Special-purpose software: MATLAB functions for estimation of peaks from time series. National Institute of Standards and Technology, http://www.itl.nist.gov/div898/winds/peakest_files/peakest.htm
- Main, J.A. and Fritz, W.P. (2006), “Database-assisted design for wind: concepts, software, and examples for rigid and flexible buildings”, NIST Building Science Series 180, National Institute of Standards and Technology, Technology Administration, US Department of Commerce.
- Mann, J. (2012), Atmospheric turbulence. DTU Wind Energy, Technical University of Denmark, Denmark, DK-4000 Roskilde. ftp://breeze.colorado.edu/pub/RSWE/Jakob_Mann.pdf
- Mann, J., Kristensen, L. and Jensen, N.O. (1998), “Uncertainties of extreme winds, spectra, and coherences”, in *Bridge Aerodynamics*, (Eds., Larsen, A. and Esdahl, S.), 49-56.
- Mann, M.E. and Emanuel, K.A. (2006), “Atlantic hurricane trends linked to climate change”, *EOS. Trans. Am. Geophys. Union*, **87**(24), 233-241.
- NIST (2016), NIST aerodynamic database [WWW Document]. <http://fris2.nist.gov/winddata/>
- Sadek, F. and Simiu, E. (2002), “Peak non-gaussian wind effects for database-assisted low-rise building design”, *J. Eng. Mech. - ASCE*, **128**, 530-539. doi:10.1061/(ASCE)0733-9399(2002)128:5(530)
- Sagaut, P. (2006), *Large Eddy Simulation for Incompressible Flows: An Introduction*. 3rd Ed., Springer.
- Scanivalve (2016), ZOC33 Service Manual. Liberty Lake, WA. www.scanivalve.com
- Simiu, E. (2011), *Design of Buildings for Wind – A Guide for ASCE 7-10 Standard Users and Designers of Special Structures*. 2nd Ed. John Wiley & Sons, Inc., NY.
- Simiu, E. and Scanlan, R.H. (1996), *Wind effects on Structures: Fundamentals and Applications to Design*. Wiley, New York.
- Stathopoulos, T. and Surry, D. (1983), “Scale effects in wind tunnel testing of low buildings”, *J. Wind Eng. Ind. Aerod.*, **13**, 313-326. doi:10.1016/0167-6105(83)90152-6
- Tieleman, H.W., Surry, D. and Mehta, K.C. (1996), “Full/model-scale comparison of surface pressures on the Texas Tech experimental building”, *J. Wind Eng. Ind. Aerod.*, **61**, 1-23. doi:10.1016/0167-6105(96)00042-6
- Turbulent Flow 2015. Getting Started: Series 100 Cobra Probe. <http://www.turbulentflow.com.au/Downloads/Getting Started - Cobra Probe.pdf>